

Moving from millifluidic to truly microfluidic sub-100- μm cross-section 3D printed devices

Michael J. Beauchamp¹ · Gregory P. Nordin² · Adam T. Woolley¹

Received: 15 March 2017 / Revised: 28 April 2017 / Accepted: 5 May 2017 / Published online: 13 June 2017
© Springer-Verlag Berlin Heidelberg 2017

Abstract Three-dimensional (3D) printing has generated considerable excitement in recent years regarding the extensive possibilities of this enabling technology. One area in which 3D printing has potential, not only for positive impact but also for substantial improvement, is microfluidics. To date many researchers have used 3D printers to make fluidic channels directed at point-of-care or lab-on-a-chip applications. Here, we look critically at the cross-sectional sizes of these 3D printed fluidic structures, classifying them as millifluidic (larger than 1 mm), sub-millifluidic (0.5–1.0 mm), large microfluidic (100–500 μm), or truly microfluidic (smaller than 100 μm). Additionally, we provide our prognosis for making 10–100- μm cross-section microfluidic features with custom-formulated resins and stereolithographic printers. Such 3D printed microfluidic devices for bioanalysis will accelerate research through designs that can be easily created and modified, allowing improved assays to be developed.

Keywords Microfluidics/microfabrication · Separations/instrumentation · Bioanalytical methods

Introduction

Three-dimensional (3D) printing has quickly gained acclaim as a technology with the potential to revolutionize

manufacturing and scientific research. It is a technique whereby a physical object is created from a digital design file. The object is generally made by a printer one layer at a time on the basis of the printing method and algorithms in the printer software that determine where to form solid material according to the design and certain user specifications. This method of creating structures allows rapid iterative changes in design to be made and then fabricated, which is one reason why 3D printing is sometimes referred to as rapid prototyping. This ability to quickly change or edit designs also allows varied structures to be made without the expensive and time-consuming processes involved in forming new masters, templates, or molds in conventional micromachining. Indeed, 3D printed fluidic devices can be made in a modular manner with individual components linked together in various configurations to create working devices from multiple pieces [1–4]. In addition to facilitating rapid prototyping, 3D printing can provide an automated process wherein a complete device is made with essentially no operator input in the manufacturing process, reducing time and training requirements. Following fabrication, potentially simple postprocessing steps such as resin clearing or support removal are all that need to be done to make a device ready for use.

3D printing holds considerable potential value for analytical chemists, as varied, custom-designed miniaturized parts can be made rapidly and with low costs. A key advantage of 3D printing is that it has a much lower cost barrier to entry than conventional cleanroom-based techniques for microfabrication that require expensive equipment and extensive training. These features motivated researchers to use 3D printing to create fluidic structures for analytical applications and to desire to make 3D printed microfluidic devices. Microfluidics offers advantages over traditional analytical platforms, including lower reagent consumption and waste generation, integration and automation of processes, and

✉ Adam T. Woolley
atw@byu.edu

¹ Department of Chemistry and Biochemistry, Brigham Young University, C100 BNSN, Provo, UT 84602, USA

² Department of Electrical and Computer Engineering, Brigham Young University, Provo, UT 84602, USA

portability. Perhaps one of the greatest potential advantages 3D printing could offer microfluidics is the possibility of making complex 3D fluidic networks much more easily than with use of stacked, two-dimensional surface micromachined layers. 3D printing can also allow simplified interfacing of devices with external fluid sources, as threaded ports [5, 6] and Luer-lock systems [2, 7, 8] have been printed as part of fluidic devices. Finally, 3D printing design files can be shared easily, which should facilitate collaboration and enable broad use.

Numerous reviews of 3D printing of sub-millimeter-scale fluidics have been published in recent years [2, 3, 9–14], describing types of printers, and configurations and applications of devices. Here, we discuss improving resolution significantly to 3D print truly microfluidic (less than 100- μm cross-section) structures. We focus less on a general overview of 3D printing, thus allowing us to give a more detailed evaluation of current and future needs to make truly microfluidic channel sizes beyond the current possibilities. 3D printing of fluidic features typically uses one of three approaches: polyjet (PJ), stereolithography (SLA), or fused deposition modeling (FDM).

PJ printers use a sprayer to deposit droplets of resin, which are cured by UV light; successive layers are then formed and cured on top of each previous layer. To make fluidic structures PJ printing requires the use of a sacrificial support material for imbedded channels or voids, so the next layer can be deposited on top. PJ printing has approximately 25- μm resolution for positioning of the print head and can form devices from two or more component inks; however, a key challenge for PJ-printed fluidics is the difficulty in effectively removing the sacrificial support materials from fluidic channels. Examples of PJ printers include the Projet 3000HD and Objet 30.

FDM is a method that uses a thermoplastic that is extruded through a heated nozzle in patterned layers, which after cooling and hardening give a device. FDM generally prints quickly but suffers from lower resolution (approximately 50 μm for print head placement, but typical nozzle extrusion diameters and layer heights are hundreds of micrometers) than either PJ printing or SLA. FDM has the benefit of being able to print different materials because multiple print heads can be incorporated at the same time. Additionally, if stopping and restarting printing at specified times is feasible, multiple materials such as glass coverslips or semipermeable membranes can be introduced during the process. Examples of FDM printers include the Stratasys Dimension Elite and Makerbot Replicator.

SLA uses a vat of liquid resin that is photopolymerized typically with LED light patterned by a projector or a scanned laser that determines the spatial resolution. In SLA, patterned interior voids for fluids contain unpolymerized liquid resin that must be flushed after fabrication. This process is much easier than for either PJ printing or FDM since the unpolymerized resin is a liquid (and low-viscosity resins can be made). In theory, SLA resolution for fluidic structures is

limited in current commercial 3D printers by the projector pixel size to approximately 30 μm , but in practice polymerization in subsequent layers typically limits channel cross sections to approximately 500 μm . Examples of SLA printers include the Miicraft and Asiga Pico Plus. A subcategory of SLA is two-photon polymerization (TPP). TPP 3D printing uses a scanned laser instead of an LED and projector as the light source and has very high resolution (approximately 1 μm) [15–17]. Unfortunately, multiple fundamental limitations of TPP hinder its application in the making of microfluidic devices. For example, because each voxel must be individually addressed, print times can be as long as 10 h per cubic millimeter. Moreover, TPP 3D printers typically cost hundreds of thousands of US dollars, making them cost-prohibitive for many research applications. These price/size/time constraints severely limit TPP 3D printing to niche, very high resolution applications, rather than construction of microfluidic analysis devices.

In this review we look critically at the sizes of fluidic channels that have been 3D printed and focus on the general characteristics of the printers in which they were made. We further specify terminology to properly classify device dimensions as millifluidic (larger than 1 mm), sub-millifluidic (0.5–1.0 mm), large microfluidic (100–500 μm), or microfluidic (smaller than 100 μm). The cutoff of 100 μm for microfluidic features follows the consensus 100-nm definition for nanoscale structures [18]. We note that the size scale achieved with most current 3D printing techniques is better classified as millifluidic rather than microfluidic. Indeed, current 3D printed fluidics are too large for microchip capillary electrophoresis, organ-on-chip vasculature, and many types of single-cell analyses. We first examine fluidic features on the exterior of 3D printed devices and describe the benefits and downsides of creating these structures and subsequently laminating a layer to make enclosed fluidic features. Next we look at 3D printed fluidic features on the interior of devices and examine the size regimes reached as well as the pros and cons of this approach. We then outline directions forward for 3D printing of microfluidics with cross sections less than 100 μm , including improvements in materials and types of printers.

Printing external features

We first examine 3D printed devices that have features on the exterior of the print, and which require a postprint lamination process to make enclosed fluidic structures. Table 1 gives an overview of published work, providing minimum feature sizes in the X/Y and Z directions, either as described in the publications or in some cases as inferred from figures and scale bars. Table 1 further gives the brand of printer used and its resolution specifications, print time (where provided), and the application or use of the prints.

The first group of surface 3D printed features are rather large (greater than millimeter scale), and are classified as millifluidic once channels are enclosed. Brooks et al. [19] made devices smoothed by exposure to tetrahydrofuran for 1 min and sealed through attachment to a polydimethylsiloxane piece to study secretions from endocrine tissue with temporal resolution. Mandon et al. [20] looked at printing hydrogels with embedded enzymes to set up sequences of reactions; importantly, they demonstrated the use of multiple materials with SLA. Takenaga et al. [21] monitored H⁺ concentrations by photocurrent detected in cultured cells by sealing their device and sandwiching it between a silicon chip and a glass coverslip. However, having at least one dimension larger than 1 mm limits the potential applications of these fluidic devices.

The next group of 3D printed surface feature devices are all sub-millifluidic, having their smallest dimension 500 μm or greater. Hamad et al. [22] made a 3D printed device for cyclic voltammetry; they measured pressure and bonding limits, and sealed their devices to a flexible plate with an adhesive ink. Monaghan et al. [23] used 3D printed trenches to test optical fiber combinations and configurations to monitor reaction

progress by UV–vis absorption. Figure 1 shows a photograph of a device with fluidic channels, grooves to function as holders for optical fibers, and threaded connectors. Using the rapid fabrication advantages of 3D printing, they were able to test several different widths and depths of channels as well as integrate threaded connections for the off-chip flow system. Additionally, they used online monitoring in their device to optimize reaction temperature and residence time. These sub-millifluidic devices have smaller features than the previous group, but are still too large for many small-volume applications.

The next group of 3D printed surface device features have large microfluidic dimensions between 100 and 500 μm, and a postprint lamination or enclosure step is needed to create the fluidic structures. Kise et al. [24] 3D printed a spacer that was sealed with two glass slides to make a passive continuous flow mixer with integrated UV–vis, fluorescence, and mid-IR spectroscopic probes. To make nutrient-rich hydrogel spheres, Alessandri et al. [25] 3D printed a concentric conical nozzle that was interfaced with various solution inputs and allowed them to create concentric shells inside the spheres. Although these prints are approaching the 100 μm size range for typical

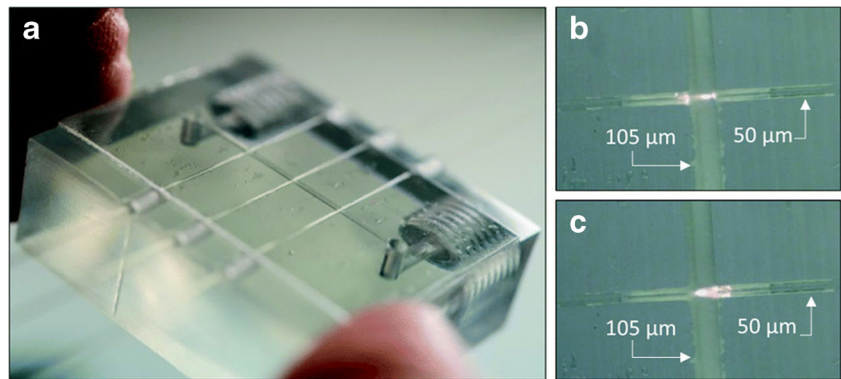
Table 1 3D printed devices with exterior fluidic features

Minimum Feature Size	Printer	Print time	Printer resolution specifications	Reference	Application
X/Y	Z				
2 mm	Makerbot Replicator 2		100 μm Z	[19]	Multispoke device to measure temporally resolved secretion from cells
1 mm	B9 Creator		101 μm Z, 50 μm X/Y	[20]	3D printed hydrogels with embedded enzymes
4.3 mm	1 mm	Asiga Pico Plus		[21]	Detected photocurrent to find H ⁺ concentration in cultured cells
800 μm	700 μm	Miicraft Onmijet 300	50 μm Z	[22]	3D printed system for cyclic voltammetry
25 μm	500 μm	3D Systems Viper Si2	50 μm Z, 75-μm beam diameter	[23]	Optical fiber configurations for UV–vis monitoring of reactions
	200 μm	Tepetier-Host		[24]	Passive continuous flow mixer with integrated spectroscopic probes
200 μm	Pico 27	40 min	27 μm X/Y	[25]	Concentric nozzle to make spheroids of nutrient-rich hydrogels
100 μm	50 μm	Inkjet Projet HD 3500 Plus	30 μm X/Y	[4]	Detection of alpha fetoprotein
100 μm	50 μm	Projet HD 3500 Plus	16 μm Z, 25 μm X/Y	[26]	Comparison of PJ and SLA fabrication for zebrafish embryo optical analysis
		3D Systems Viper Pro	50 μm Z, 25 μm X/Y		
		Projet 7000HD	50 μm Z, 25 μm X/Y		
130 μm	20 μm	Ultimaker 2	50 μm Z, 300 μm X/Y	[27]	Micro free flow electrophoresis
	50 μm	D3 Projet 1200	25 μm Z, 500 μm X/Y	[28]	Device to monitor blood hemoglobin concentration with a smartphone
50 μm	Ultimaker 2		400-μm extruder nozzle	[29]	Paused printing to add coverslips, membranes, optical components

Entries are sorted approximately according to feature size, with those having the largest features listed at the *top*.

PJ polyjet, SLA stereolithography

Fig. 1 Example of a 3D printed device with external features laminated to form fluidic structures. **a** Image of a completed device. **b, c** Configuration of optical fibers; feature sizes are listed. (Adapted with permission from [23], *arrows* added for clarity)



microfluidic applications, they still require postprocessing steps to seal the channels that are formed only on the device exterior.

The smallest category of these devices have feature sizes less than $100\ \mu\text{m}$ on the exterior of the print. Lee et al. [4] made channels $50\ \mu\text{m}$ tall and $100\ \mu\text{m}$ in the X/Y direction in a device for the detection of alpha fetoprotein. PJ and SLA 3D printers were compared by Zhu et al. [26]; they sealed their channels with a $500\text{-}\mu\text{m}$ -thick optically transparent plate and studied zebrafish embryos to determine resin biocompatibility. Anciaux et al. [27] created a free flow electrophoresis device with shallow ($20\text{-}\mu\text{m}$) fluidic features that were sealed to a separate 3D printed piece in an acetone vapor bath. As an application to point-of-care diagnostic tools, Plevniak et al. [28] developed a 3D printed device that was sealed to a glass slide and holder to monitor blood hemoglobin levels with use of smartphone camera detection. A final example is from Yuen [29], who used FDM to create structures, but paused at specific points to add objects to the print, such as coverslips, thin films, membranes, and optical components. Devices in this category have channel sizes appropriate for a range of microfluidic analyses, but are limited by posttreatment processes to seal the channels and further fail to take advantage of the full device volume and utility afforded by 3D printing.

These examples show that surface features can be printed with dimensions appropriate for microfluidic applications. However, important unresolved issues remain for printing channels on the exterior of devices. First, because the features are on the surface of the print, they do not become fluidic structures until they are fully enclosed with another piece. This lamination process can be done through solvent-assisted methods, heated presses, or tape or clamps to attach pieces from either the same material as the printed resin or another material such as glass. Notably, these bonding steps increase fabrication complexity and introduce potential errors or complications that can occur because of a two-material seam, where delamination or leakage is possible. Even more importantly, creation of channels exclusively on the exterior of prints suffers from all the inherent issues of surface micromachining and its inability to make truly 3D structures.

In contrast, the ability to create truly microfluidic features throughout a solid object volume in all three dimensions with use of 3D printing would provide a revolutionary advance over lithography-based cleanroom methods.

Printing internal fluidic features

Here, we focus on fluidic features printed fully within the interior of a device, as summarized in Table 2. The minimum channel size is defined as the smallest fluidic feature successfully printed and through which solution could flow. Table 2 also gives the brand of printer used and its resolution specifications (if provided in the reference), the time for the print, and a description of the application(s) of the 3D printed fluidic structures. Although fluidic channels formed within the interior of a 3D print avoid many of the problems associated with making fluidic features on the device exterior, new issues arise in creating these structures. A key concern is the postprint removal of material left inside the channels during printing. For PJ and FDM printers a separate sacrificial material is deposited to complete the planar layer and allow the device material to be printed on this surface in the next print layer (otherwise it would fill in the intended fluidic features below). This sacrificial material and its removal step limit the feature sizes that can be produced. In addition, for FDM prints the size of the printer nozzle and the process by which the liquid material is allowed to cool limit resolution, because a line of liquid resin spreads out before it cools and hardens to the desired shape. In SLA the unpolymerized liquid resin within the channels must be flushed to create fluidic structures; this unpolymerized SLA liquid resin can be removed easily with an applied vacuum, especially when low-viscosity resins are used. A visual representation of the mismatch between printer resolution specifications and 3D print results is shown in Fig. 2. The 3D printed interior channel cross-sectional areas are all more than an order of magnitude larger than the minimum feasible dimension predicted by printer specifications alone. This plot demonstrates the need for caution in

Table 2 3D printed interior fluidic features and applications

Minimum feature size		Printer	Print time	Printer resolution specifications	Reference	Application
<i>X/Y</i>	<i>Z</i>					
>1 mm		Projet HD 3500 Plus		30 μm	[4]	Fluidic components for alpha fetoprotein detection
>1 mm		Projet 3000 HD	4–6 h	32 μm <i>Z</i> , 38.6 μm <i>X/Y</i>	[30]	Fluidic capacitors, transistors, and diodes
3 mm	1.5 mm	Objet Connex 350		Droplet size 42 μm	[6]	Monitored drug transport with cells
1 mm	1 mm	Miicraft		56 μm <i>X/Y</i> , 50 μm <i>Z</i>	[31]	Tested viscosity and adulterants in milk
500 μm	1 mm	Miicraft		100 μm <i>Z</i> , 50 μm <i>X/Y</i>	[32]	Components for protein quantitation
1 mm	300 μm	Illios 3D printer	30 min	12.5 μm <i>Z</i> , 51 μm <i>X/Y</i>	[33]	Biocompatible resin for cell culture
800 μm	800 μm	Form 1+			[5]	Incorporated electrodes to detect DNA
500 μm	750 μm	Fineline Prototyping service			[1]	Modular design of connected components
650 μm	650 μm	Form 1+		10- μm laser spot	[34]	DNA ligation and PCR
250 μm	250 μm	Shapeways ultra HD service		100 μm <i>Z</i> , 25 μm <i>X/Y</i>		
600 μm	600 μm	Form 1+			[35]	3D printed droplet generator
500 μm	500 μm	Ultimaker 2 and Miicraft		100 μm <i>Z</i>	[36]	Droplet generator for cell encapsulation
500 μm	500 μm	Felix 3.0	6 min	50 μm <i>Z</i> , 300 μm <i>X/Y</i>	[37]	Comparison of FDM, PJ, and SLA printers
250 μm	250 μm	Eden 260 VS	30 min	16 μm <i>Z</i> , 250 μm <i>X/Y</i>		
150 μm	150 μm	Miicraft+	12 min	50 μm <i>Z</i> , 56 μm <i>X/Y</i>		
500 μm		Miicraft		50 μm <i>Z</i> , 50 μm <i>X/Y</i>	[34]	Mixing for pK_a determination in an external instrument
500 μm		3D Systems Viper SL			[7]	Bacterial detection in food using antibodies and magnetic beads
500 μm		Perfactory Minimultilense		32 μm <i>X/Y</i> , 30 μm <i>Z</i>	[38]	Array of droplet generators for monodisperse microgels
250 μm	250 μm	Miicraft		30 μm <i>Z</i> , 56 μm <i>X/Y</i>	[39]	Comparison of SLA, PJ, and FDM printers in making fluidic channels
		ProJet 3500 HD Max		16 μm <i>Z</i> , 25 μm <i>X/Y</i>		
		Objet 260 Connex		16 μm <i>Z</i> , 20 μm <i>X/Y</i>		
250 μm		Miicraft DMD	12 min to 6 h	50 μm <i>Z</i> , 50 μm <i>X/Y</i>	[40]	Mixer, droplet generator for nitrite detection
200 μm	200 μm	Object Eden350V		178 μm <i>Z</i>	[41]	Comparison of print results for PJ and FDM
200 μm	200 μm	Projet 3000 HD		38 μm <i>X/Y</i> , 16 μm <i>Z</i>	[42]	UV-vis monitoring of beverages
200 μm	200 μm	Projet 3000 HD		16 μm <i>Z</i>	[43]	Droplet generator, statistics on droplet sizes
300 μm	150 μm	B9 Creator	40 min	50 μm <i>Z</i>	[44]	Active microfluidic valves
162 μm	150 μm	Asiga PicoPlus	1 h	27 μm <i>X/Y</i> , 1 μm <i>Z</i>	[45]	Multiplexed pump and valve system
108 μm	60 μm	Asiga PicoPlus		27 μm <i>X/Y</i> , 1 μm <i>Z</i>	[46]	Resin optimization to print truly microfluidic channels

Entries are sorted approximately according to feature size, with those having the largest features listed at the *top*.

FDM fused deposition modeling, *PJ* polyjet, *SLA* stereolithography

predicting minimum fluidic feature dimensions from printer resolution specifications, as well as the importance of both pushing achievable feature sizes closer to printer resolution specifications and improving printer resolution.

First we discuss 3D printed internal millifluidic features with cross sections in at least one dimension larger than 1 mm. Lee et al. [4] 3D printed millifluidic modules that were connected to make a device for the detection of alpha fetoprotein. Sochol et al. [30] reported 3D printing of millifluidic capacitors, diodes, and transistors. A millifluidic device created by Anderson et al. [6] monitored drug transport in cells on a membrane that was interfaced with 3D printed channels. Figure 3 shows a device photograph and schematic design. This device had threaded fittings to directly connect it to a syringe pump and mass spectrometer, allowing the concentration of drug delivered to the cells to be determined, and cell viability could be probed by fluorescence. Venkateswaran

et al. [31] developed an SLA-printed millifluidic device to determine the viscosity of milk and thus the concentration of adulterants. A number of manually operated millifluidic components, such as pumps and valves, were printed by Chan et al. [32] for a disposable, point-of-care analysis unit for total protein quantification in urine. Urrios et al. [33] 3D printed millifluidic channels using a biocompatible polyethylene glycol diacrylate SLA resin. Although the millifluidic features within the interior of the devices reported in all these articles took advantage of the 3D nature of prints, the millimeter-scale channel cross sections were too large for many analysis applications.

Most 3D printed interior channels are in the sub-millifluidic range (0.5–1.0 mm), which can be made to work for select analyses, but is still limiting for many analytical applications. A device with incorporated electrodes to detect DNA via $[\text{Ru}(\text{bpy})_3]^{2+}$ (where bpy is 2,2'-bipyridyl) was

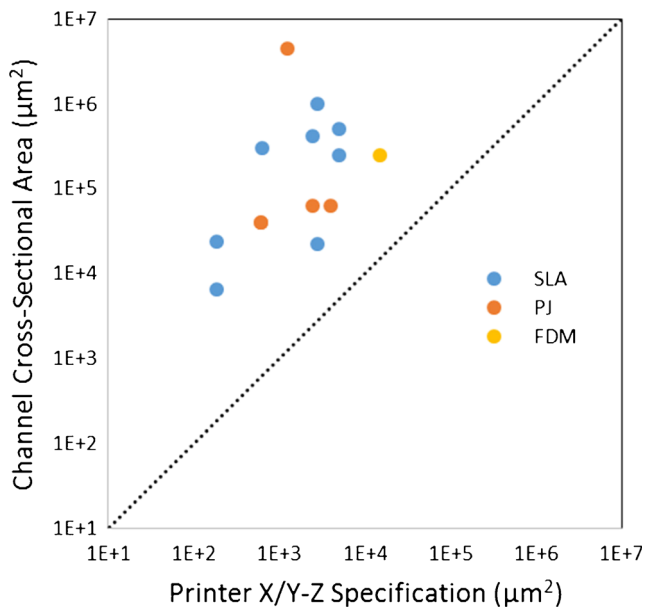


Fig. 2 Achieved internal 3D printed fluidic channel cross-sectional areas as a function of printer resolution specifications. The printer X/Y resolution is multiplied by the step size Z to give the printer $X/Y-Z$ specification. *FDM* fused deposition modeling, *PJ* polyjet, *SLA* stereolithography

printed by Bishop et al. [5]. A commercial printing service was used to make a variety of components that were hooked together in a modular design allowing Bhargava et al. [1] to produce a droplet generator and mixers to control flow rates. DNA reactions, including PCR, were performed by Patrick et al. [34] in another commercially made device. An FDM printer was used to create a droplet generator that had 600- μm channels and an adjustable screw that could control

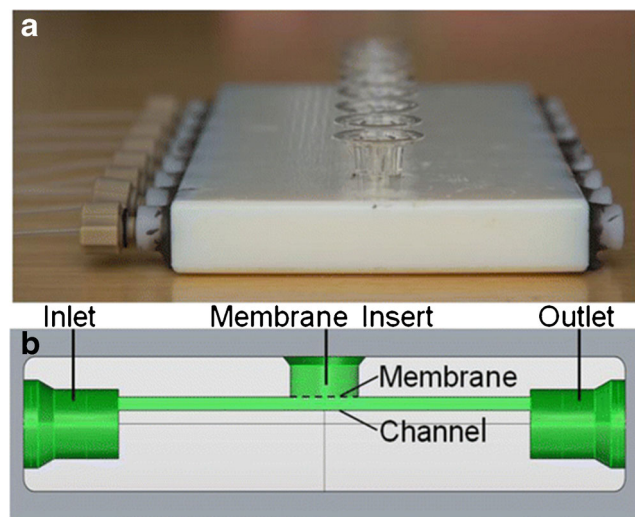


Fig. 3 A 3D printed device used to study drug effects on cells. **a** Photograph of a device connected to input/output lines. **b** The side view of the design. (Reprinted with permission from [6]. Copyright 2013 American Chemical Society)

the droplet size [35]. Morgan et al. [36] reported a droplet generator with 500- μm -diameter channels, which were used to encapsulate dental pulp stem cells and determine viability. A 3D printed device was made by Lee et al. [7] for detection of bacteria in foods using antibodies attached to magnetic beads. In an interesting application, Femmer et al. [38] took advantage of 3D capabilities to create an array of droplet generators using 500- μm channels to create emulsions and microgels. Devices with channels having at least one dimension between 0.5 and 1 mm in the interior begin to leverage 3D printed fluidic capabilities, but are still too large to be useful in a range of microfluidic analysis applications.

Large 3D printed internal microfluidic features have dimensions between 100 and 500 μm , which makes available additional analysis capabilities but still does not allow the full range of microfluidic applications. Shalhan et al. [40] created a 3D printed micromixer and droplet generator in a device for nitrite detection with channels as small as 250 μm . Four different PJ printers were tested by Walczak and Adamski [42] for the minimum channel size they could make; the fluidic devices were used for UV-vis analysis of beverages, and the prints were evaluated for fidelity, conformity, and roughness. They found that removal of support material limited the minimum feature size that could be made. A droplet generator was made via PJ printing that could form droplets of different sizes; their theoretical and experimental sizes were compared, and the polydispersity index of the droplets was determined [43].

A few recent articles have directly compared different 3D printing techniques to examine their performance, although without a focus on a specific chemical or biological application. Ukita et al. [39] made a centrifugal fluidic concept device with interior channels as small as 250 μm on a side. They also examined the fidelity of prints for a given design size and the smoothness of a sloped surface; from these results they estimated 200 μm to be the minimum feasible channel dimension. A second article compared PJ and FDM printer resolution, accuracy, circularity, biocompatibility, roughness, and water contact angle [41]. Minimum interior channel dimensions of approximately 200 μm were created; PJ printing offered higher spatial accuracy and smoother features than FDM, whereas objects made with both printers had good biocompatibility. Finally, very recent work by Macdonald et al. [37] compared the use of SLA, PJ, and FDM printers to create Y-shaped microfluidic devices having interior fluidic channel sizes as small as 150 μm with SLA fabrication. They evaluated surface roughness, fidelity, mixing of two input streams, postprocessing steps, and device cost. They determined that FDM printers offer a range of materials and low costs; PJ printers have high fabrication throughput but are expensive and interior channels are difficult to clear; and although SLA printers have lower throughput, they offer the smoothest and best-defined channels, with short postprocessing times and good laminar flow properties.

Our recent publications show sizes in or near the true microfluidic range for 3D printed devices having fluidic pumps and valves that withstand more than 1,000,000 actuations without breaking [44]. Figure 4 shows a 3D printed pump based on multiple valves made with a custom-formulated SLA resin [45]. This multiplexer was able to direct fluid flow from any of three possible inputs into either of two available outputs, and the channel cross-sectional features were smaller than 200 μm . We have recently 3D printed truly microfluidic (approximately $100 \times 100 \mu\text{m}^2$ cross section) channels using SLA [46]. We optimized the concentration of UV absorber in the resin, and compared our microfluidic structures with the sub-millifluidic ones made by several commercial 3D printing services. In addition to being able to produce smaller channels, our custom formulation of resins allows careful control of the surface or bulk device properties, including elasticity and chemistry. These truly microfluidic devices now available with SLA 3D printing open the door to performing microchip electrophoresis, probing single cells, forming vasculature mimics, creating laminar flow mixers, forming monoliths for analyte retention, etc.

Outlook

3D printing of millifluidic structures is routine, and although many authors misclassify such devices as microfluidic, there is clearly an urgent, unmet need for similar capabilities in 3D printing of truly microfluidic features smaller than 100 μm . Such sub-100- μm 3D printed microfluidic structures would have sufficiently small channels to perform novel lab-on-a-chip operations not accessible with current 3D printed devices. To achieve these lofty goals, which are just now becoming feasible with the smallest microfluidic 3D prints [45, 46], sub-100- μm fluidic features are essential. In the near term, 3D printing of sub-100- μm microfluidics will likely need to be done via SLA, because of the difficulty and tedious nature of removing solid sacrificial supports required for making fluidic structures by PJ printers and insufficient resolution in FDM. In theory, PJ and FDM printing could achieve truly microfluidic interior channel sizes with improved support materials for PJ systems or smaller nozzles/new configurations for FDM printers. If support material removal, smoothness, and resolution obstacles to printing truly microfluidic features by FDM or PJ printing are overcome, then their unique capabilities, such as embedding materials during printing in FDM or printing with several materials via PJ, could be fully leveraged. Likewise, printing fluidic features only on the device exterior and later sealing them introduces complications, including of risk of delamination, increased fabrication time and complexity, and limitations in sophistication of fluidic networks.

SLA 3D printers are the only ones to have made approximately 100 μm internal microfluidic structures to date [46],

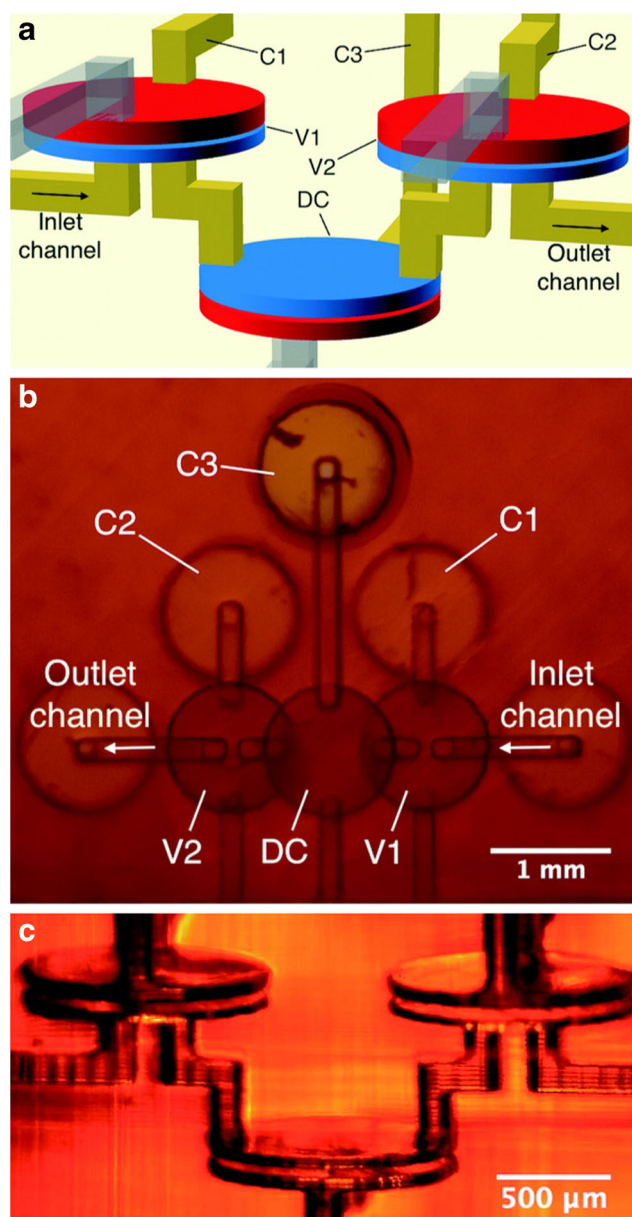


Fig. 4 Microfluidic pumps and valves. **a** Valves and a displacement chamber that make a pumping unit. **b** Top-view photograph of a printed pump with multiple inputs. **c** Photograph of a pump with the same orientation as the schematic in (a). (Reprinted from [45])

and are presently best suited to further push the size limit of 3D printing. Moreover, SLA prints comprise a single, complete piece with no need for bonding of secondary components; the only requirement is to flush the unpolymerized resin with a vacuum or by flowing solvent. Smooth channel surfaces offered by SLA facilitate laminar flow [34], and recent work further demonstrates the potential for creating multimaterial SLA prints [20]. An additional feature of SLA 3D printing is the ability to create new resins and fine-tune existing ones, offering the ability to have individual components adjusted or optimized to suit a user's needs. Indeed, the ability to custom formulate resins has been crucial to our

success in creating approximately 100 μm fluidic features as well as pumps and valves [45, 46]. We [47], and more recently others [33], have shown that devices made from polyethylene glycol diacrylate are desirable for biocompatibility, including reduced adsorption of protein to surfaces and cell viability.

As researchers continue to push the limit from approximately 100 μm to the 10 μm fluidic size scale in 3D prints, custom resin formulations easily interfaced with SLA printers will be essential. Further improvements in SLA projector resolution and optics to yield approximately 2 μm pixels will aid in the drive toward 10 μm features. Fully incorporating 3D and truly microfluidic systems in easily formed devices will be a crucial step in the advancement of lab-on-a-chip technology. 3D printing allows these designs to be optimized iteratively in a low-cost manner and opens the possibility to create novel and more advanced 3D structures. We further envision that new materials will provide microscale active components in novel 3D architectures for biochemical analyses. The development of such 3D printed, truly microfluidic systems should have a major impact on bioanalytical science.

Acknowledgements We are grateful to the US National Institutes of Health (R01 EB006124) for partial support of this work.

Compliance with ethical standards

Conflict of interest The authors declare that they have no conflict of interest.

References

- Bhargava KC, Thompson B, Malmstadt N. Discrete elements for 3D microfluidics. *Proc Natl Acad Sci U S A*. 2014;111:15013–8.
- Chen C, Mehl BT, Munshi AS, Townsend AD, Spence DM, Martin RS. 3D-printed microfluidic devices: fabrication, advantages and limitations—a mini review. *Anal Methods*. 2016;8:6005–12.
- Amin R, Knowlton S, Hart A, Yenilmez B, Ghaderinezhad F, Katebifar S, et al. 3D-printed microfluidic devices. *Biofabrication*. 2016;8:022001.
- Lee KG, Park KJ, Seok S, Shin S, Kim DH, Park JY, et al. 3D printed modules for integrated microfluidic devices. *RSC Adv*. 2014;4:32876–80.
- Bishop GW, Satterwhite-Warden JE, Bist I, Chen E, Rusling JF. Electrochemiluminescence at bare and DNA-coated graphite electrodes in 3D-printed fluidic devices. *ACS Sens*. 2016;1:197–202.
- Anderson KB, Lockwood SY, Martin RS, Spence DM. A 3D printed fluidic device that enables integrated features. *Anal Chem*. 2013;85:5622–6.
- Lee W, Kwon D, Chung B, Jung GY, Au A, Folch A, et al. Ultrarapid detection of pathogenic bacteria using a 3D immunomagnetic flow assay. *Anal Chem*. 2014;86:6683–8.
- Au KA, Lee W, Folch A. Mail-order microfluidics: evaluation of stereolithography for the production of microfluidic devices. *Lab Chip*. 2014;14:1294–301.
- He Y, Wu Y, Fu J, Gao Q, Qiu J. Developments of 3D printing microfluidics and applications in chemistry and biology: a review. *Electroanalysis*. 2016;28:1–22.
- Huang Y, Leu MC, Mazumder J, Donmez A. Additive manufacturing: current state, future potential, gaps and needs and recommendations. *J Manuf Sci Eng*. 2015;137:014001.
- Yazdi AA, Popma A, Wong W, Nguyen T, Pan Y, Xu J. 3D printing: an emerging tool for novel microfluidics and lab-on-a-chip applications. *Microfluid Nanofluid*. 2016. doi:10.1007/s10404-016-1715-4.
- Waheed S, Cabot JM, Macdonald NP, Lewis T, Guijt RM, Paull B, et al. 3D printed microfluidic devices: enablers and barriers. *Lab Chip*. 2016;16:1993–2013.
- Bhattacharjee N, Urrios A, Kang S, Folch A. The upcoming 3D-printing revolution in microfluidics. *Lab Chip*. 2016;16:1720–42.
- Au AK, Huynh W, Horowitz LF, Folch A. 3D-printed microfluidics. *Angew Chem Int Ed*. 2016;55:3862–81.
- Engelhardt S, Hoch E, Borchers K, Meyer W, Krüger H, Tovar G, et al. Fabrication of 2D protein microstructures and 3D polymer-protein hybrid microstructures by two-photon polymerization. *Biofabrication*. 2011;3:025003.
- Raimondi MT, Eaton SM, Laganà M, Aprile V, Nava MM, Cerullo G, et al. Three-dimensional structural niches engineered via two-photon laser polymerization promote stem cell homing. *Acta Biomater*. 2013;9:4579–84.
- Claeysens F, Hasan EA, Gaidukeviciute A, Achilleos DS, Ranella A, Reinhardt C, et al. Three-dimensional biodegradable structures fabricated by two-photon polymerization. *Langmuir*. 2009;25:3219–23.
- Klaessig F, Marrapese M, Abe S. Current perspectives in nanotechnology terminology and nomenclature. In: Murashov V, Howard J, editors. *Nanotechnology standards*. New York: Springer; 2011. p. 21–52.
- Brooks JC, Fort KI, Holder DH, Holtan MD, Easley CJ. Macro to micro interfacing to microfluidic channels using 3D printed templates: application to time resolved secretion sampling of endocrine tissue. *Analyst*. 2016;141:5714–21.
- Mandon CA, Blum LJ, Marquette CA. Adding biomolecular recognition capability to 3D printed objects. *Anal Chem*. 2016;88:10767–72.
- Takenaga S, Schneider B, Erbay E, Biselli M, Schnitzler T, Schoning MJ, et al. Fabrication of biocompatible lab on chip devices for biomedical applications by means of a 3D printing process. *Phys Status Solidi A*. 2015;212:1347–52.
- Hamad EM, Bilatto SER, Adly NY, Correa DS, Wolfrum B, Schöning MJ, et al. Inkjet printing of UV curable adhesive and dielectric inks for microfluidic devices. *Lab Chip*. 2016;16:70–4.
- Monaghan T, Harding MJ, Harris RA, Friel RJ, Christie SDR. Customizable 3D printed microfluidics for integrated analysis and optimization. *Lab Chip*. 2016;16:3362–73.
- Kise DP, Reddish MJ, Dyer RB. Sandwich format 3D printed microfluidic mixers: a flexible platform for multi probe analysis. *J Micromech Microeng*. 2015;25:124002.
- Alessandri K, Feyeux M, Gurchenkov B, Delgado C, Trushko A, Krause KH, et al. A 3D printed microfluidic device for production of functionalized hydrogel microcapsules for culture and differentiation of human neuronal stem cells. *Lab Chip*. 2016;16:1593–604.
- Zhu F, Skommer J, Macdonald NP, Friedrich T, Kaslin J, Wlodkowic D. Three dimensional printed millifluidic devices for zebrafish embryo tests. *Biomicrofluidics*. 2015. doi:10.1063/1.4927379.
- Anciaux SK, Geiger M, Bowser MT. 3D printed micro free flow electrophoresis device. *Anal Chem*. 2016;88:7675–82.
- Plevniak K, Campbell M, Myers T, Hodges A, He M. 3D printed auto-mixing chip enables rapid smartphone analysis of anemia. *Biomicrofluidics*. 2016. doi:10.1063/1.4964499.
- Yuen PK. Embedding objects during 3D printing to add new functionalities. *Biomicrofluidics*. 2016. doi:10.1063/1.4968909.

30. Sochol RD, Sweet E, Glick CC, Venkatesh S, Avetisyan A, Ekman KG, et al. 3D printed microfluidic circuitry via multijet based additive manufacturing. *Lab Chip*. 2016;16:668–78.
31. Venkateswaran PS, Sharma A, Dubey S, Agarwal A. Rapid and automated measurement of milk adulteration using a 3D printed optofluidic microviscometer (OVM). *IEEE Sens J*. 2016;16:3000–7.
32. Chan HN, Shu Y, Xiong B, Chen Y, Chen Y, Tian Q, et al. Simple, cost effective 3D printed microfluidic components for disposable, point of care colorimetric analysis. *ACS Sens*. 2016;1:227–34.
33. Urrios A, Parra-Cabrera C, Bhattacharjee N, Gonzalez-Suarez AM, Rigat-Brugarolas LG, Nallapatti U, et al. 3D printing of transparent bio-microfluidic devices in PEGDA. *Lab Chip*. 2016;16:2287–94.
34. Patrick WG, Nielsen AA, Keating SJ, Levy TJ, Wang CW, Rivera JJ, et al. DNA Assembly in 3D printed fluidics. *PLoS One*. 2015. doi:10.1371/journal.pone.0143636.
35. Zhang JM, Li EQ, Aguirre-Pablo AA, Thoroddsen ST. A simple and low cost fully 3D printed non planar emulsion generator. *RSC Adv*. 2016;6:2793–9.
36. Morgan AJL, San Jose LH, Jamieson WD, Wymant JM, Song B, Stephens P, et al. Simple and versatile 3D printed microfluidics using fused filament fabrication. *PLoS One*. 2016. doi:10.1371/journal.pone.0152023.
37. Macdonald NP, Cabot JM, Smejkal P, Guit RM, Paull B, Breadmore MC. Comparing microfluidic performance of three-dimensional (3D) printing platforms. *Anal Chem*. 2017;89:3858–66.
38. Femmer T, Jans A, Eswein R, Anwar N, Moeller M, Wessling M, et al. High throughput generation of emulsions and microgels in parallelized microfluidic drop makers prepared by rapid prototyping. *ACS Appl Mater Interfaces*. 2015;7:12635–8.
39. Ukita Y, Takamura Y, Utsumi Y. Direct digital manufacturing of autonomous centrifugal microfluidic device. *Jpn J Appl Phys*. 2016;55:06GN02.
40. Shallah AI, Smejkal P, Corban M, Guijt RM, Breadmore MC. Cost effective 3D printing of visible transparent microchips within minutes. *Anal Chem*. 2014;86:3124–30.
41. Lee JM, Zhang M, Yeong WY. Characterization and evaluation of 3D printed microfluidic chip for cell processing. *Microfluid Nanofluid*. 2016;20:5.
42. Walczak R, Adamski K. Inkjet 3D printing of microfluidic structures-on the selection of the printer towards printing your own microfluidic chips. *J Micromech Microeng*. 2015;25:085013.
43. Donvito L, Galluccio L, Lombardo A, Morabito G, Nicolosi A, Reno M. Experimental validation of a simple, low cost, T junction droplet generator fabricated through 3D printing. *J Micromech Microeng*. 2015;25:035013.
44. Rogers CI, Qaderi K, Woolley AT, Nordin GP. 3D printed microfluidic devices with integrated valves. *Biomicrofluidics*. 2015;9:016501.
45. Gong H, Woolley AT, Nordin GP. High density 3D printed microfluidic valves, pumps, and multiplexers. *Lab Chip*. 2016;16:2450–8.
46. Gong H, Beauchamp M, Perry S, Woolley AT, Nordin GP. Optical approach to resin formulation for 3D printed microfluidics. *RSC Adv*. 2015;5:106621.
47. Rogers CI, Pagaduan JV, Nordin GP, Woolley AT. Single-monomer formulation of polymerized polyethylene glycol diacrylate as a nonadsorptive material for microfluidics. *Anal Chem*. 2011;83:6418–25.